Borneo International Journal of Biotechnology (BIJB)
Vol. 1 (December 2020), 103 – 123

e-ISSN 2716-697X

Research Article

OPTIMISATION OF AN ELECTROCHEMICAL SENSOR BASED ON BARE GOLD ELECTRODE FOR DETECTION OF ALUMINIUM ION

Gilbert Ringgit[1], Shafiquzzaman Siddiquee[1*], Suryani Saallah[1] and Mohammad Tamrin Mohamad Lal[2]

[1]Biotechnology Research Institute, Universiti Malaysia Sabah, Kota Kinabalu, Sabah, Malaysia
[2]Borneo Research Marine Institute, Universiti Malaysia Sabah, Kota Kinabalu, Sabah, Malaysia
*Corresponding author's email: shafiqpab@ums.edu.my
Received date: 2 January 2020 | Accepted date: 22 May 2020

ABSTRACT

In this work, an electrochemical method for detection of trace amount of aluminium (Al^{3+}), a heavy metal ion, based on a bare gold electrode (AuE) was developed. Current responses of the AuE under various type of electrolytes, redox indicators, pH, scan rate and accumulation time were investigated using cyclic voltammetry (CV) method to obtain the optimum conditions for Al^{3+} detection. The sensing properties of the AuE towards the target ion with different concentrations were investigated using differential pulse voltammetry (DPV) method. From the CV results, the optimal conditions for the detection of Al^{3+} were Tris-HCl buffer (0.1 M, pH 2) supported by 5 mM Prussian blue with scan rate and accumulation time respectively of 100 mVs^{-1} and 15 s. Under the optimum conditions, the DPV method was detected with different concentrations of aluminium ion ranging from 0.2 to 1.0 ppm resulted in a good linear regression r^2 = 0.9806. This result suggests that the optimisation of the basic parameters in electrochemical detection using AuE is crucial before further modification of the Au-electrode to improve the sensitivity and selectivity especially for the low concentration of ion detection. The developed method has a great potential for rapid detection of heavy metal ion (Al^{3+}) in drinking water samples.

Keywords: electrochemical sensor, heavy metal, aluminium, cyclic voltammetry, differential pulse voltammetry

INTRODUCTION

Aluminium is the most abundant metal in the Earth's crust that can be found in a wide variety of chemical forms throughout the environment. Aluminium has been used tremendously in industrial applications for fabrication of electrical appliances, automobiles, building constructions, packaging materials, cooking utensils as well as for the development of vaccines (Mergu, Singh, & Gupta, 2015; Soni, White, Flamm, & Burdock, 2001; Baylor, Egan, & Richman, 2002). Besides, aluminium is a well-known flocculant in the water treatment system. The high amount of aluminium from human daily activities could be changed the amount of aluminium in the environment. The concentrated aluminium is entering the environment through the raining process. The pH of the rain is changed more to the acidic condition as aluminium high released into the air. As a result, acidic raining condition high amount of aluminium is saturated in natural water and biological systems (Tripathi et al., 2014; Manjumeena, Duraibabu, Rajamuthuramalingam, Venkatesan, & Kalaichelvan, 2015).

Excessive exposure to this metal element has been linked to serious health problems related to neurodegenerative and neurological disorders such as Alzheimer's disease (Rastogi, Dash, & Ballal, 2017), Parkinson's disease and dementia (Ramezani, Jahani, Mashhadizadeh, Shahbazi, & Jalilian, 2018), breast cancer (Kim, Angupillai, & Son, 2016) and other diseases like osteomalacia (Kim et al., 2016; Sarkar, Ghosh, Gharami, Mondal, & Murmu, 2017). Therefore, accurate determination and efficient monitoring of aluminium level in the food chain, especially the drinking water system has become increasingly important. An average safety level of weekly human body dietary intake of aluminium is 7 mg kg^{-1} body weight while the permissible level in drinking water is 0.2 ppm as per WHO guidelines (Diao et al., 2016; Fu et al., 2014; Barceló & Poschenrieder, 2002; WHO, 2008).

Several analytical methods for the aluminium detection in different matrices are available such as fluorescence method (Manjumeena et al., 2015), flame atomic absorption spectrometry (Altunay, Yıldırım, & Gürkan, 2018), graphite furnace atomic absorption spectrometry (Dravecz, Bencs, Beke, & Gali, 2016), flow injection/sequential injection analysis (Khanhuathon, Siriangkhawut, Chantiratikul, & Grudpan, 2015), inductively coupled plasma mass spectrometry (Silva et al., 2015), near-field enhanced atomic emission spectroscopy (Wang et al., 2018), inductively coupled plasma dynamic reaction cell mass spectroscopy (Skalny et al., 2018), UV-vis spectroscopy (Lima, Papai, & Gaubeur, 2018; Elečková, Alexovič, Kuchár, Balogh, & Andruch, 2015), neutron activation analysis (Mohseni et al., 2016) and high-performance liquid chromatography (Zioła-Frankowska, Kuta, & Frankowski, 2015). However, most of these methods are complicated, time-consuming, and required skilled operators to perform the *ex-situ* analysis (Ma, Yuan, Chai, & Liu, 2010; Rana, Mittal, Singh, Singh, & Banks, 2017; Suherman et al., 2018).

In recent years, electrochemical techniques for determination of aluminium are a subject of immense interest by researchers worldwide as a simple and rapid alternative to the aforementioned conventional methods. On top of that, an advanced method allowed for the fabrication of portable device via *in situ* analysis (Suherman et al., 2018; Ramezani et al., 2018). In electrochemical sensing, selection of suitable working electrode is important as it has a direct impact on the current formation. Among the various type of working electrodes for electrochemical sensing applications, gold electrode offers favourable characteristics in terms of electrocatalytic and conductive properties, good selectivity, high signal to noise ratio, and have been widely used for detection of varying heavy metal ions including ions of hexavalent chromium (Wu et al., 2019), arsenite (Wen, Wang, Yuan, Liang, & Qui, 2018), mercury (Yang et al., 2015), cadmium and lead (Xuan & Park, 2018; Gumpu, Veerapandian, Krishnan, & Rayappan, 2017) as well as zinc and manganese ions (Gilbert et al., 2018, Gilbert, Siddiquee, Saallah, & Tamrin, 2019). However, in most cases of electrochemical sensing based on Au-electrode, the electrode is simply used, modify and functionalised for detection of the target ion. As the current response obtained during the electrochemical measurement is highly influenced by various factors such as types of the electrolytic solution, redox indicators, pH, scan rates and accumulation times, investigation of the effect of these factors towards the current response is of great importance to obtain the optimum conditions that can give a good current response. To the best of our knowledge, there is no paper published on the optimisation of the electrochemical method for aluminium ion detection using a bare gold electrode.

MATERIALS AND METHODS

Chemicals for preparation of buffer including potassium hydrogen phosphate, potassium dihydrogen phosphate, sodium citrate dihydrate and sodium chloride were purchased from Systerm while sodium citrate dihydrate and citric acid anhydrous were obtained from Nacalai Tesque. The other buffer materials including hydrochloric acid, ammonium acetate and Tris-HCl were purchased respectively from J. T. Baker, Ajax Chemical and FIRST Base. The chemicals of redox indicator were obtained from Nacalai Tesque (potassium hexacyanoferrate (III) and potassium ferrocyanide (II) trihydrate), Systerm (methylene blue) and Sigma-Aldrich (iron (III) chloride). Aluminium sulphate as a target ion was obtained from Systerm.

Instrumentation

All electrochemical measurements were carried out using a potentiostat/galvanostat (PGSTAT) electrochemical workstation (Metrohm-Autolab B.V) with a standard three-electrode system consisting of a bare gold electrode, platinum wire and silver chloride as the working, counter and reference electrodes, respectively. Voltammograms obtained from the CV and DPV methods were analysed with NOVA Autolab 1.11 software. All experiments were conducted at a room temperature condition of 20 ± 2°C.

Pre-treatment of the Bare Gold Electrode

The bare AuE pre-treatment was conducted according to the method previously described by Siddiquee, Yusof, Salleh, Tan, and Bakar (2010). First, the working electrode (gold) was polished with alumina slurry (0.3 – 0.5 µm in diameter) for 2 minutes followed by subsequent cleaning and rinsing with distilled water. Then, the electrode was dried using nitrogen gas before submerged together with the counter electrode (platinum) and the reference electrode (silver chloride) in 3 M potassium chloride (KCl) solution. These three electrodes were used to measure the current flows through the electrolytic solution after applying the potential (external current).

Preparation of the Electrolytic Solutions

Five types of electrolytic buffer solutions were studied including acetate buffer (Chaiyo et al., 2016; Honeychurch, Rymansaib, & Iravani, 2018), phosphate buffer saline (Gholivand, Akbari, Faizi, & Jafari, 2017; Trachioti, Hrbac, & Prodromidis, 2018), citrate buffer (Gumpu et al., 2017), ammonium buffer (Ferancová, Hattuniemi, Sesay, Räty, & Virtanen, 2016) and Tris-HCl buffer (Ensafi, Amini, & Rezaei, 2013). The mentioned buffers were prepared in 0.1 M concentration. These buffers were widely used for the detection of heavy metal ions.

Preparation of the Redox Indicators

Three redox indicators including plusferocyanide ($[Fe(CN_6)]^{4-}$) (Peng et al., 2016), methylene blue (MB) (Ensafi et al., 2013) and Prussian blue (PB) (Wen et al., 2018) were investigated to 'boost' the current response and improve the performance of the bare AuE. These redox indicators were dropped onto the surface of the electrode and left for 2 minutes to allow attachment on the surface of the electrode. The concentrations of

all redox indicators were standardised to 5 mM for 10 µL. Then, these redox indicators were applied for the detection of aluminium ions. The combination of the matched buffer with redox indicator is shown in Scheme 1 with the current response.

Preparation of the Al^{3+} Analyte

The concentration of Al^{3+} was set at 0.2 ppm according to the standard drinking water quality by WHO (2008) and Engineering Service Division, Ministry of Health, Malaysia (2016). A 0.2 ppm of aluminium sulphate ($Al_2(SO_4)_3$) was diluted directly into 10 mL of buffer solution under 100 mVs^{-1} with potential volt ranging from 0.0 to 1.7 V for CV measurements. Five different buffers were tested at 0.2 ppm of Al in the presence of three redox indicators. For the DPV procedure, different concentrations of aluminium ion were detected from 0.2 to 1.0 ppm.

A 10 µL of (5 mM) redox indicator was dropped onto the surface of the Au electrode and left for 2 minutes. Then, the electrode was cleaned with Tris-HCl buffer solution before the electrochemical measurement. In this procedure, all electrodes (working electrode, the counter electrode and reference electrode) were submerged into 10 mL of buffer solution containing 0.2 ppm of aluminium ion. The setting of optimal electrochemical measurements such as the potential range from 0.0 V to 1.7 V; stop and start potential = 0.8 V; scan rate = 100 mVs^{-1} under 15 s of accumulation time. These measurements were determined through optimisation step using the CV method. The DPV method was performed at different concentrations of Al^{3+}.

RESULTS AND DISCUSSION

To obtain the best results for Al^{3+} detection using bare AuE, selection of electrochemical conditions including types of buffer and redox indicators, pH, scan rates and accumulation times are crucial as these conditions have a direct impact to the current signals during electrochemical measurement. Therefore, in this study, these parameters were studied and optimised using the CV method and applied for detection with different concentrations of Al^{3+} using the DPV method.

Selection of Buffer and Redox Indicator

Electrolytic solutions consisted of both the positively-charged (cation) and negatively-charged (anion) ions. Generally, the positive charge ion attracts to the negative terminal while the negative charge ion moves to a different direction (positive terminal). When an external force is applied in the form of potential, the current travels into different medium known as an electrolytic solution. The medium with the presence of the charged ions capable to conduct the electricity and exhibited the formation of current in the form of voltammogram graph.

In this study, five types of buffer were tested as electrolytic solution as these buffers have been used by other researchers for detecting varying heavy metal ions such as zinc (Honeychurch et al., 2018), cadmium (Trachioti et al., 2018; Gumpu et al., 2017), arsenite (Gumpu et al., 2017), lead (Tarley et al., 2017), mercury (Gumpu et al., 2017), nickel (Ferancová et al., 2016). Effect of the buffer towards the electrochemical detection of aluminium ion is depicted in cyclic voltammograms as shown in Figure 1. Tris-HCl buffer supported by 5 mM Prussian blue (PB) showed the highest peak current responses as compared to other buffers and redox indicators. The magnitude of oxidation almost twice was higher than that of the reduction which indicated that the two ion radicals were diffused onto the surface-active area by competition process (Rana et al., 2017).

The oxidation peak formed at 1.6130 V (3.6907 mA) while the reduction was formed at 0.4704 V with the current response of –0.9821 mA. The formations of the peak for all buffers are not in a position of potential range. All the peaks were shifting from one to another. This shifting of current responses was due to the diffusion of the aluminium ion on the surface of the bare AuE. Based on the current responses, Tris-HCl buffer supported by 5 mM Prussian blue was selected as an electrolytic solution for detection of Al^{3+}.

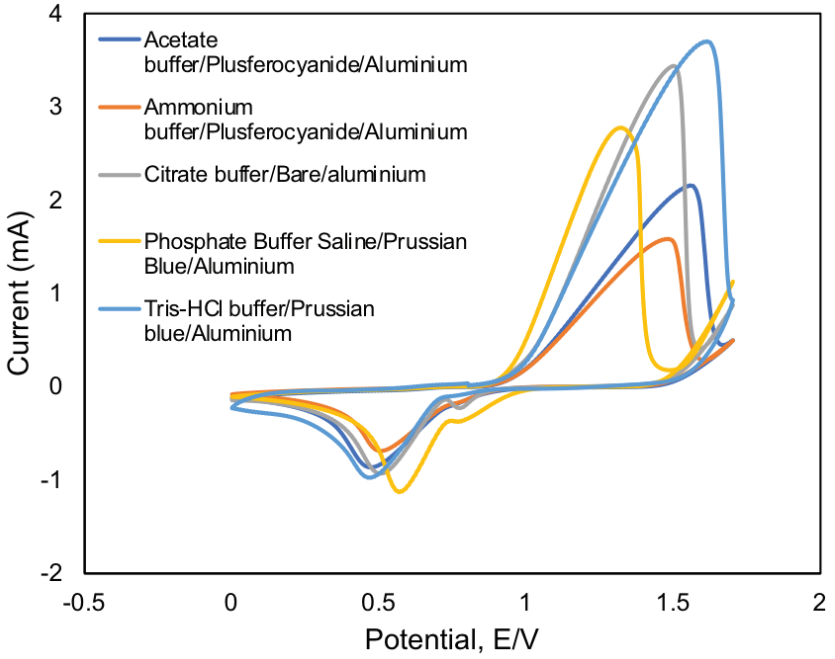

Figure 1 CV analysis of different buffers (0.1 M, pH 2) in the presence of 5 mM redox indicators. The buffers such as acetate buffer, ammonium buffer, citrate buffer, phosphate buffer saline and Tris-HCl buffer tested with potential range from 0.0 V to 1.7 V and 100 mVs^{-1} scan rates. The experimental work was repeated at least three times (n>3)

Effects of the Different pH Ranges

The influence of the pH of the electrolytic solutions on the detection of Al^{3+} was studied by CV in the presence of 0.2 ppm of Al^{3+} in 0.1 M Tris-HCl buffer supported by 5 mM Prussian blue, with pH values ranging from 2.0 to 9.0 (Figure 2A). The pH value was calibrated using either 1 M hydrochloric acid (HCl) or 1 M potassium hydroxide (KOH). The cyclic voltammograms were obtained under the potential ranged from 0.0 to 1.7 V.

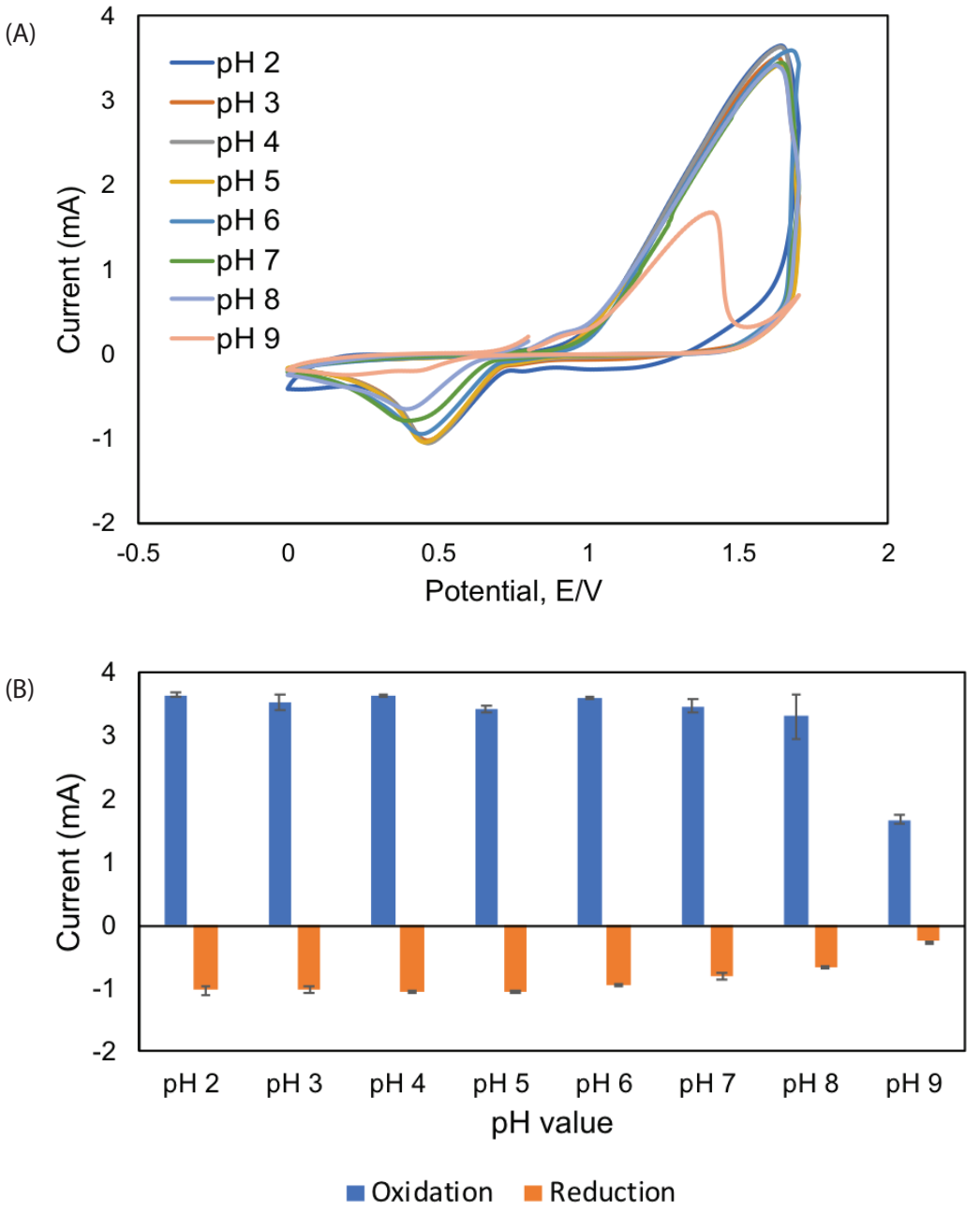

Figure 2 CV analysis for optimisation of the pH values for pH 2 to 9. The optimisation of pH was applied to 0.1 M Tris-HCl buffer supported by 5 mM Prussian blue in the presence of 0.2 ppm Al^{3+}. The graph of different pH values 2(A) and the comparison of oxidation and reduction peaks for every peak point formed on 2(B). The repetition of the experiment was conducted more than three times (n>3)

Based on Figure 2(A), there was no much different on the current response on oxidation and reduction reactions. Therefore, the comparison of the current response was evaluated based on the peak current responses by oxidation and reduction peak current signals in Figure 2(B). Oxidation and reduction peaks were formed with different potential ranged of 0.0 V to 1.7 V. Oxidation peaks were formed at more positive potential point at 1.6227 V to 1.6768 V while reduction closed to 0.0 V specifically potential point between 0.3947 V to 0.4655 V. At this potential, electron flowed at the highest potential rate as indicated by the highest peak signal before its declining to form a horizontal line where the equilibrium state of both oxidation and reduction current located. Overall, the oxidation peaks were always higher than the reduction peaks for all the pH value assay. At the reduction peak, pH 2 until pH 5, almost similar current responses were obtained. Above pH 5, the current responses were gradually decreased. As for the oxidation peak, at pH 2 to pH 8, the current responses were fluctuated and rapidly declining at pH 9. The pH 2 (Tris-HCl buffer) was selected as the optimal pH as both oxidation and reduction peak currents obtained maximum value.

Effects of Scan Rate

The effects of scan rate were evaluated using the CV method by adjusting the rate of current flow in the system in the electrochemical measurement. Electrochemical measurement for scan rate analysis was performed as 50 mVs^{-1}, 100 mVs^{-1}, 150 mVs^{-1} and 200 mVs^{-1} as shown in Figure 3(A). Based on Figure 3, the current signal getting higher as the scan rate adjusted at a higher value.

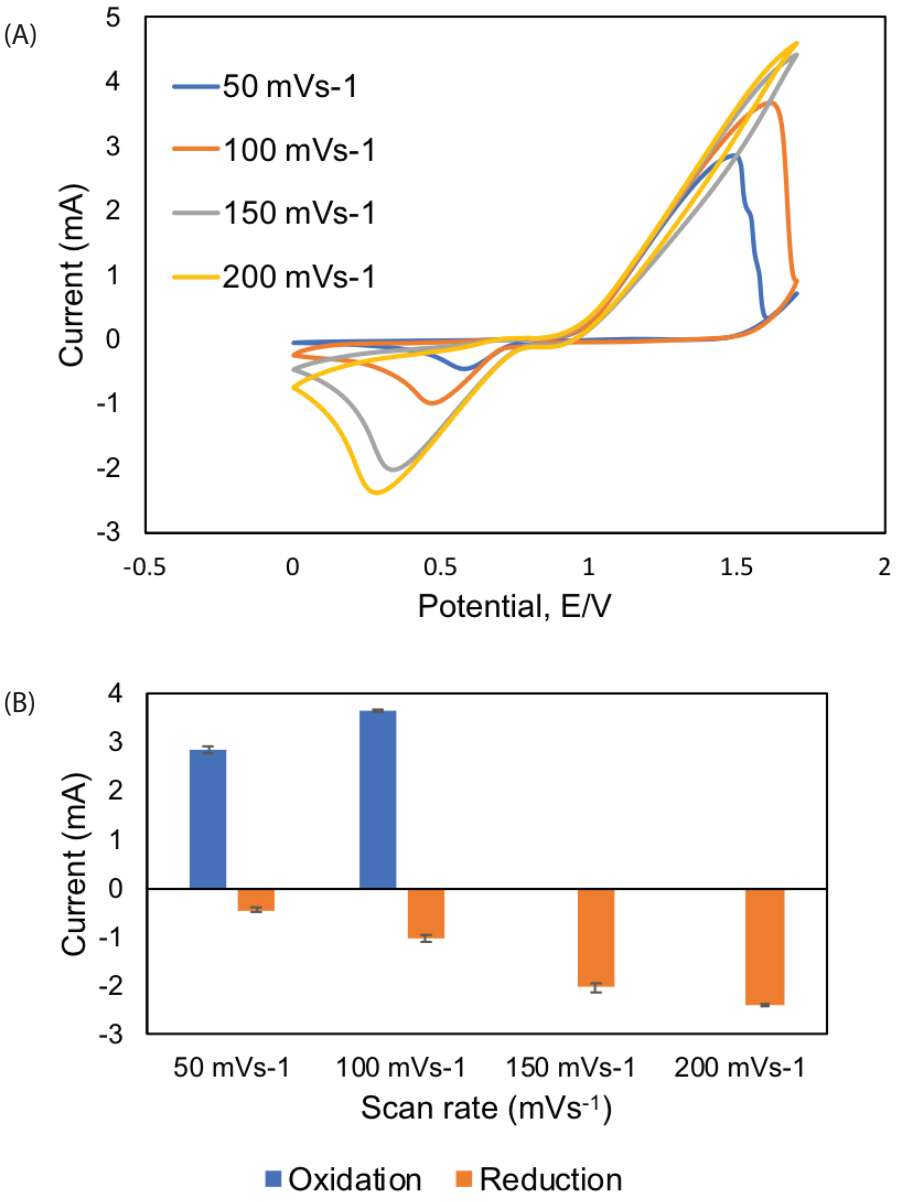

Figure 3 CV analysis for optimisation of scan rate from 50, 100, 150 and 200 mVs^{-1} for (0.1 M, pH 2) Tris-HCl buffer supported by 5 mM Prussian blue with the presence of 0.2 ppm Al^{3+}. The graph for different scan rates (A) and line graph of the comparison between oxidation and reduction potential peaks current response (B). This experiment was conducted more than three times (n>3)

This indicated that scan rate proportions to peak current signal. According to Suherman et al. (2018), this formation was due to surface controlled of bare AuE to aluminium ion based on the shifted graph. Absorption of the aluminium ion was depending on the speed of the current flow promoted by the scan rate. The faster the current flow, the higher the current response as shown by the 100 mVs^{-1} scan rate until overoxidation occurred when the scan rate above 100 mVs^{-1} was applied. Oxidation peaks with a scan rate of 150 mVs^{-1} and 200 mVs^{-1} were invalid due to the flat current response as the speed of the current increased. Despite the validity, the scan rate of 50 mVs^{-1} and 100 mVs^{-1} were left to compare. From Figure 3(B), it was seen that the 100 mVs^{-1} scan rate has higher oxidation and reduction peaks compared to the 50 mVs^{-1} scan rate. Therefore, 100 mVs^{-1} was chosen as the optimal scan rate for this study.

Effects of Accumulation Time

The effects of accumulation time on electrochemical detection of Al^{3+} was investigated using the CV method. Before analysis began, the accumulation time was applied to allow the current flow into the system first by generating the current to breakdown the chemical compounds into single radial ions such as cation and anion. These ions were transferred into the cathode and anode as a result of oxidation and reduction peaks current as shown in Figure 4(A). The range of accumulation was selected from 5 – 40 s. All the accumulation times showed not many different responses except for the 10 s, where the current response dropped drastically (Figure 4(B)).

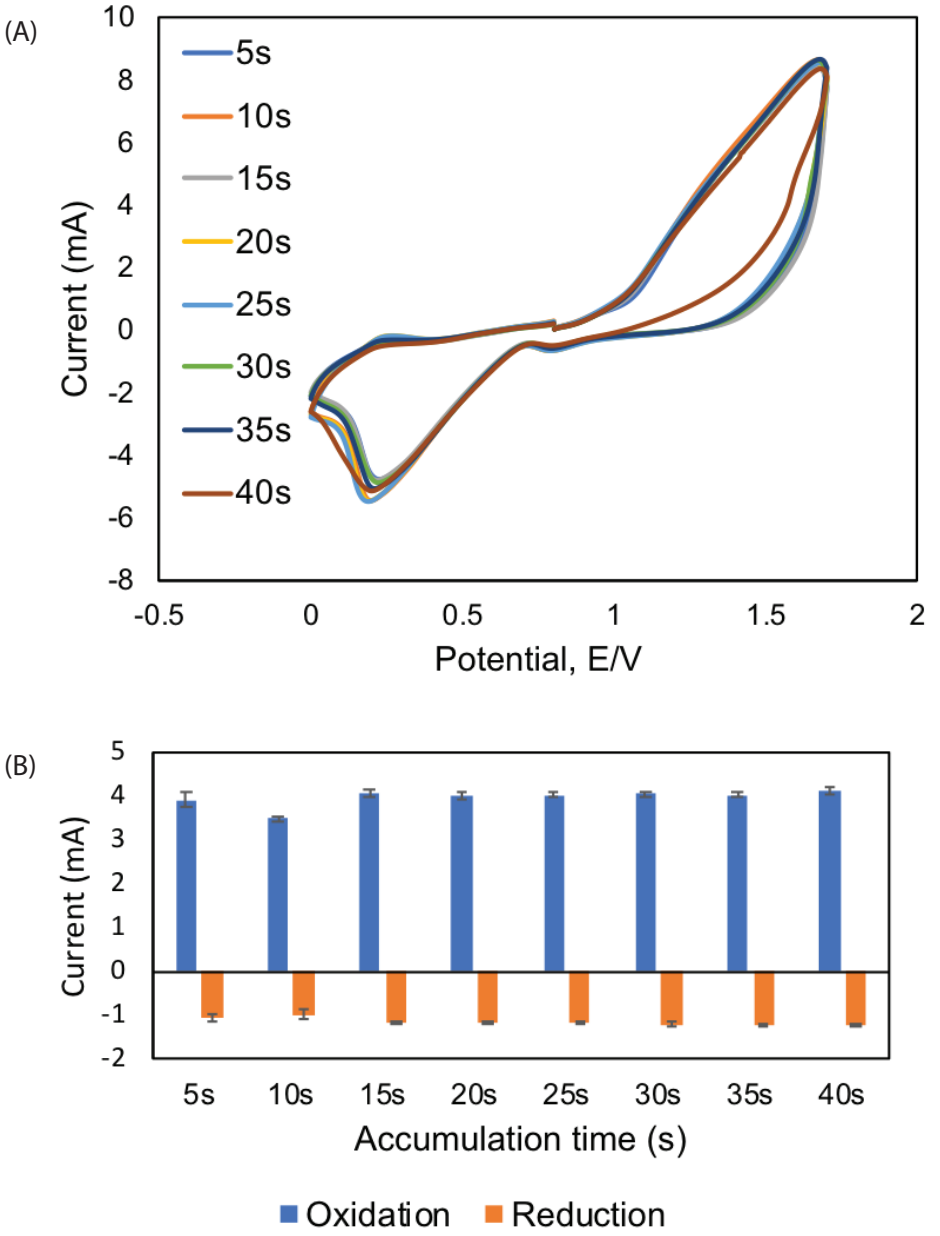

Figure 4 CV analysis for optimisation of the accumulation time from 5, 10, 15, 20, 25, 30 and 40 s for (0.1 M, pH 2) Tris-HCl buffer supported by 5 mM Prussian blue at the presence of 0.2 ppm aluminium under 100 mVs^{-1} of scan rate. The graph of different accumulation times (A) and the line graph for oxidation and reduction peaks formed by cyclic voltammogram. This experiment was conducted at least three times (n> 3)

At this accumulation time, the lowest current response at oxidation and reduction peaks were obtained as compared to the other accumulation times. Theoretically, this factor might be due to the net charge concentration and surface-active site. According to the Nernst-Planck equation:

$$\frac{\partial C_i}{C_t} + \vec{\mu} \cdot \nabla C_i \left(\nabla \cdot \vec{\mu}_i\right) = D_i \nabla^2_{C_i}$$

Where is the electric current, is the diffusion coefficient, gradient concentration and is ionic strength. When the current as experiencing momentum due to diffusion coefficient and gradient concentration of the current (, it is expressed as:

$$i = -D \nabla C_i$$

Based on the equation, Al^{3+} experienced the repulsion force as it approaches the surface of the electrode due to the similar positive charge of both the ion and the electrode. This statement leads to the second condition, as aluminium ion experienced momentum, has convicted its electrons. As aluminium lost 3 electrons, aluminium oxidized into Al^{3+}. The 3 electrons are forced transferring to the bare AuE which Au^{3+} under 100 mVs^{-1} of scan rate. Its force against the electromagnetic force produced by different terminal charges with the presence of external force such as current for a non-spontaneous chemical reaction to occur. The concentration of its current, then, expressed as:

$$i_{con} = \mu_i C_i$$

Where is ionic strength and is the concentration of the aluminium (Wang, 2001). The second factor might be happened was due to surface active site. The current signal was depending on the absorption site capacity according to Langmuir isotherm as shown below:

$$\emptyset = \frac{KP_A}{1 + KP_A} = \frac{\text{No. adsorption site occupied}}{\text{No. adsorption site available}}$$

As the rate of adsorption was while the rate desorption was . The equilibrium reaction between the rate of adsorption and the rate of desorption leads to the stability of the system (Wang, 2001). Therefore, 10 s showed the reaction was not fully complete in term of electron transfer and the surface-active area was still available. When the accumulation time was above 15 s, the peak of the current became stable until reaching 40 s. For the oxidation peaks, the highest current responses were observed

at a potential between 1.5 to 1.6 V due to the saturation of the ion on the electrode surface (Rana et al., 2017). A similar trend was observed at the reduction peaks where the highest current response formed at potential applied between 0.4 to 0.5 V. The selection of the 15 s was compared to other accumulation times due to sharp peak form between 10 to 15 s. This is the strong evidence of the electron transfer on the system (Rana et al., 2017). The formation of the peak from 10 to 15 s almost twice as compared the interval between the accumulation times. Therefore, 15 s was selected as an optimal accumulation time.

Detection of Different Concentration of Al^{3+}

Differential pulse voltammetry (DPV) is widely used for detection with different concentrations of Al^{3+} ranged from 0.2 to 1.0 ppm (Figure 5). After optimisation using CV analysis, DPV analysis was performed to test the current response related to different concentrations of Al^{3+} under the optimum conditions (Table 1).

Table 1 Optimum conditions applied for DPV analysis

Parameter	Optimum condition
Buffer	Tris-HCl buffer (0.1 M, pH 2)
Redox indicator	5 mM Prussian Blue
Scan rate	100 mVs^{-1}
Accumulation time	15 s
Reduction range	0.2 V to 0.8 V

The reduction range of 0.2 to 0.8 V was selected due to the stability of the current response as shown in Figure 5(A). As mentioned previously, the concentration of aluminium ion was set at 0.2 ppm according to the safety level of Al^{3+} in the drinking water standardised by Ministry of Health, Malaysia (2010) following the WHO guideline. The formation of reduction peak was observed from 0.55 to 0.75 V. The sensitivity of the bare AuE was about −0.0382 mA.

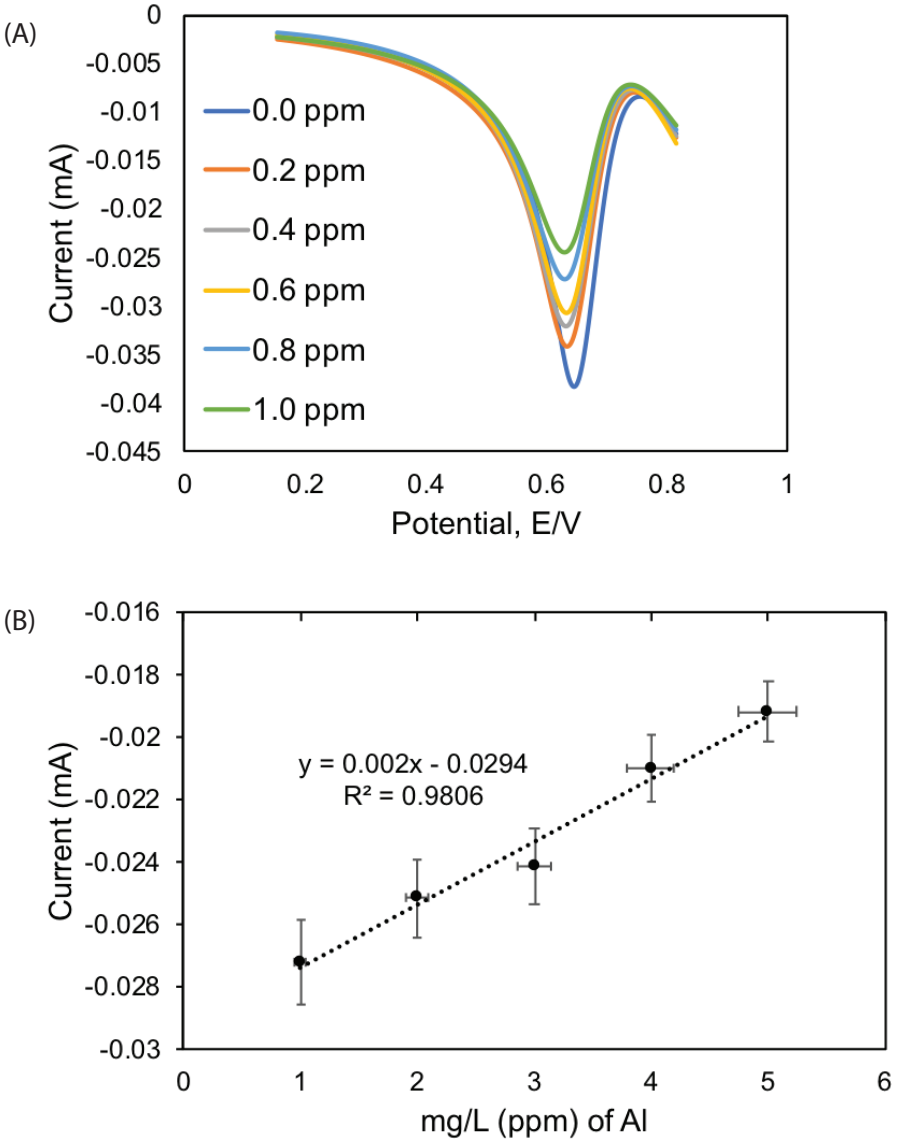

Figure 5 DPV analysis for different concentrations of aluminium in (0.1 M, pH 2) Tris-HCl buffer solution fixed as 0.2, 0.4, 0.6, 0.8 and 1.0 ppm with range potential 0.55 – 0.75 V under 100 mVs^{-1} of scan rate. DPV results of different concentrations aluminium ion (A) and the line graph for reduction peaks among the different concentrations (B). This experiment was repeated more than three times ($n > 3$)

Based on Figure 5 (A), the current is shifted to the left as the increasing amount of the aluminium added (from 0.6526 V to 0.6375 V) indicating the presence of Al^{3+} in the electrolytic solution. Also, the peak current response was proportional to the concentrations of aluminium as its approaching positive current. The peaks of the current response formed at reduction potential as the amount of the aluminium increasing. This is the strong evidence that aluminium is a strong reducing agent as its formed high peak at negative current axis according to standard reduction potential.

Determination of the reactions between the target ion and the surface of the bare AuE was conducted by analysing the data using a line graph as shown in Figure 5(B). The peak points among the concentrations were collected and the linear regression equation was obtained as $y = 0.002x - 0.0294$, where y stands for the peak of the current (mA) while x is the different concentrations of the aluminium ion (ppm) with a good linear correlation of $r^2 = 0.9806$. The peaks of the current response were closer to positive current as the high amount of aluminium added as mentioned before.

The possible electrochemical mechanism of these findings might be due to the affinity of target ion to the surface of the electrode. In the electrolytic solution, the cation produced by the buffer itself. Based on the chemical composition of Tris-HCl buffer ($C_4H_{11}NO_3$), it might produce complex compound $NH_2NaC(CH_2OH)_3.HCl$ due to the addition of sodium chloride (NaCl) into the solution. The possible chemical reaction by the formation of buffer in the electrolytic solution is as below:

$$NaCl + NH_2C(CH2OH)_3.HCl \longrightarrow NH_2NaC(CH2OH)3.HCl + Cl^-$$

Based on Alfred Werner's coordination theory, 1 HCl bound directly onto N in the form of $NH_2C(CH2OH)_3.HCl$. When the NaCl was added, the $NH_2NaC(CH2OH)_3.HCl$ was formed and it released Cl^- to bind with H^+ from water molecules (Berke, 2014). The other possible reaction was the formation of Na^+ which was possible cation that competed with Al^{3+}. This formation happened during the electrolysis process when the Na^+ breaks into the single radical ion from Tris-HCl buffer's chemical structure. The chemical reaction is shown below:

$$NH_2NaC(CH_2OH)_3.HCl \longrightarrow NH_2C(CH_2OH)_3.HCl + Na^+$$

The mixture was directly dissolved in the distilled water which was containing the cation identified as H^+. Therefore, the possible ions that might present in the solution are Na^+ are H^+ including the target ion (Al^{3+}). These ions chemically competed to attach on the cathode terminal by chemical affinity order. Theoretically, the more

positive radical ion compared to other cations, the higher chance of the ion to attach on the surface of the electrode. The affinity of Al^{3+} is stronger than H^+, while Na^+ is lower than Al^{3+} and H^+. This order might be affecting the accumulation of the ion on the surface of the bare AuE. Based on the affinity order, Al^{3+} was expected to attach on the surface of the electrode but at the same time, the Na^+ and H^+ competed on the same site which shows the unstable peak formation of different concentrations. Also, Al^{3+} was expected to attach on the surface of the electrode when the current response shifted to the left as shown in Figure 5(A). The other consideration the line graph was not linear as expected due to the charge of the electrode itself. Bare AuE has positive one ion (could be 2+ and 3+) based on it electron configuration ($5d^{10}$ $6s^1$). The repulsion force might happen between two elements with identical charges due to magnetic force. Some Al^{3+} might be repelled away from the bare AuE (positive charge) which indicated by the current responses in Figure 5(A) with less amount of aluminium shows the highest peak current response. However, the characteristic of the electrode itself as a good conductor enhanced the current flow through the system as well as increasing the current intensity cannot be denied. Therefore, the detection of Al^{3+} using AuE is successfully sensing through optimisation of all the important parameters.

CONCLUSION

This research paper reported the rapid detection of Al^{3+} using electrochemical methods through comprehensive optimisation of the important parameters such as buffer, redox indicator, pH value, scan rate, accumulation time and concentration window. The current response showed a good linear correlation (R^2 = 0.9806) with reversed current reaction, indicated by the reduction peaks when different concentrations of aluminium are applied into the DPV method. The proposed method can detect aluminium ion in 15 s. Finally, this optimised conditions, an electrochemical sensor is successfully detected of aluminium ion on the ranged of 0.2 to 1.0 ppm with high sensitivity (–0.0381663 mA). Therefore, the proposed method holds great potential for simple, rapid and in situ analysis of aluminium in drinking water and other sources.

ACKNOWLEDGEMENTS

This research was supported by UMSgreat (GUG0236-1/2018).

REFERENCES

Altunay, N., Yıldırım, E., & Gürkan, R. (2018). Extraction and preconcentration of trace Al and Cr from vegetable samples by vortex-assisted ionic liquid-based dispersive liquid–liquid microextraction prior to atomic absorption spectrometric determination. *Food Chemistry*, *245*, 586 – 594.

Barceló, J., & Poschenrieder, C. (2002). Fast root growth responses, root exudates, andinternal detoxification as clues to the mechanisms of aluminium toxicity andresistance: a review. Environmental and Experimental Botany, 48, 75–92.

Baylor, N. W., Egan, W., & Richman, P. (2002). Aluminium salts in vaccines – U.S. perspective. *Vaccine*, *20*, 18 – 23.

Berke, H. (2014). 'Counting ions' in Alfred Werner's coordination chemistry using electrical conductivity measurements. *Educación Química*, *25* (E1), 267 – 275.

Chaiyo, S., Mehmeti, E., Zagar, K., Siangproh, W., Chailapakul, O., & Kalcher, K. (2016). Electrochemical sensors for the simultaneous determination of zinc, cadmium and lead using a Na^+ion/ionic liquid/graphene composite modified screen-printed carbon electrode. *Analytica Chimica Acta*, *918*, 26 – 34.

Diao, Q., Ma, P., Lv, L., Li, T., Sun, Y., Wang, X., & Song, D. (2016). A water-soluble and reversible fluorescent probe for $Al^{3+}$and F^- in living cells. *Sensors and Actuators B*, *229*, 138 – 144.

Dravecz, G., Bencs, L., Beke, D., & Gali, A. (2016). Determination of silicon and aluminium in silicon carbide nanocrystals by high-resolution continuum source graphite furnace atomic absorption spectrometry. *Talanta*, *147*, 271 – 275.

Ensafi, A. A., Amini, M., & Rezaei, B. (2013). Detection of DNA damage induced by chromium/glutathione/H2O2 system at MWCNTs–poly (diallyldimethylammonium chloride) modified pencil graphite electrode using methylene blue as an electroactive probe. *Sensors and Actuators B: Chemical*, *177*, 862 – 870.

Elečková, L., Alexovič, M., Kuchár, J., Balogh, I. S., & Andruch, V. (2015). Visual detection and sequential injection determination of aluminium using a cinnamoyl derivative. *Talanta*, *133*, 27 – 33.

Ferancová, A., Hattuniemi, M. K., Sesay, A. M., Räty, J. P., & Virtanen, V . T. (2016). Rapid and direct electrochemical determination of Ni(II) in industrial discharge water. *Journal of Hazardous Materials*, *306*, 50 – 57.

Fu, Y., Jiang, X. J., Zhu, Y. Y., Zhou, B. J., Zang, S. Q., Tang, M. S., … Mak, T. C. W. (2014). A new fluorescent probe for Al^{3+} based on rhodamine 6G and its application to bioimaging. *Dalton Transactions*, *43*, 12624 – 12632.

Gilbert, R., Siddiquee, S., Tamrin, M. L., Saallah, S., Yusuf, N. H. M., & Amin, Z. (2018). Electrochemical methods for detection of zinc ion in drinking water. *International Journal of Pharma and Bio Science*, *9*, 268 – 276.

Gilbert, R., Siddiquee, S., Saallah, S., & Tamrin, M. L. (2019). Optimisation of parameters for detection of manganese ion using electrochemical method. *IOP Conference Series: Materials Science and Engineering*, *606*, 012009. DOI: 10.1088/1757-899X/606/1/012009

Gholivand, M. B., Akbari, A., Faizi, M., & Jafari, F. (2017). Introduction of a simple sensing device for monitoring of hydrogen peroxide based on ZnFe2O4 nanoparticles/chitosan modified gold electrode. *Journal of Electroanalytical Chemistry*, *796*, 17 – 23.

Gumpu, M. B., Veerapandian, M., Krishnan, U. M., & Rayappan, J. B. B. (2017). Simultaneous electrochemical detection of Cd (II), Pb (II), As (III) and Hg (II) ions using ruthenium (II)-textured graphene oxide nanocomposite. *Talanta*, *162*, 574 – 582.

Honeychurch, K. C., Rymansaib, Z., & Iravani, P. (2018). Anodic stripping voltammetry determination of zinc at a 3-D printed carbon nanofiber-graphite-polystyrene electrode using a carbon pseudo-reference electrode. *Sensors and Actuators B: Chemical*, *267*, 476 – 482.

Khanhuathon, Y., Siriangkhawut, W., Chantiratikul, P., & Grudpan, K. (2015). Spectrophotometric method for determination of aluminium content in water and beverage samples employing flow-batch sequential injection system. *Journal of Food Composition and Analysis*, *41*, 45 – 53.

Kim, H. S., Angupillai, S., & Son, Y. A. (2016). A dual chemosensor for both $Cu^{2+}$and Al^{3+}: A potential $Cu^{2+}$and Al^{3+}switched YES logic function with an INHIBIT logic gate and a novel solid sensor for detection and extraction of Al^{3+}ions from aqueous solution. *Sensors and Actuators B*, *222*, 447 – 458.

Lima, L. C., Papai, R., & Gaubeur, I. (2018). Butan-1-ol as an extractant solvent in dispersive liquid-liquid microextraction in the spectrophotometric determination of aluminium. *Journal of Trace Elements in Medicine and Biology*, *50*, 175 – 181.

Ma, Y. H., Yuan, R., Chai, Y. Q., & Liu, X. L. (2010). A new aluminium(III)-selective potentiometric sensor based on N,N'-propanediamide bis(2-salicylideneimine) as a neutral carrier. *Materials Science and Engineering C*, *30*, 209 – 213.

Manjumeena, R., Duraibabu, D., Rajamuthuramalingam, T., Venkatesan, R., & Kalaichelvan, P. T. (2015). Highly responsive glutathione functionalized green AuNP probe for precise colorimetric detection of Cd^{2+} contamination in the environment. *Royal Society of Chemistry Advances*, *5*, 69124 – 69133.

Mergu, N., Singh, A. K., & Gupta, V. K. (2015). Highly sensitive and selective colorimetric and off–on fluorescent reversible chemosensors for Al^{3+} based on the rhodamine fluorophore. *Sensors*, *15*, 9097 – 9111.

Engineering Service Division, Ministry of Health, Malaysia. (2016). *Drinking water quality standard*. Retrieved from https://environment.com.my/wp-content/uploads/2016/05/Drinking-Water-MOH.pdf.

Mohseni, H. K., Matysiak, W., Chettle, D. R., Byun, S. H., Priest, N., Atanackovic, J., & Prestwich, W. V. (2016). Optimization of data analysis for the in vivo neutron activation analysis of aluminium in bone. *Applied Radiation and Isotopes*, *116*, 34 – 40.

Peng, D., Hui, B., Kang, M., Wang, M., He, L., Zhang, Z., & Fang, S. (2016). Electrochemical sensors based on gold nanoparticles modified with rhodamine B hydrazide to sensitively detect Cu (II). *Applied Surface Science*, *390*, 422 – 429.

Ramezani, S., Jahani, R., Mashhadizadeh, M. H., Shahbazi, S. & Jalilian, S. (2018). A novel ionic liquid/polyoxomolybdate based sensor for ultra-high sensitive monitoring of Al(III): Optimization by Taguchi statistical design. *Journal of Electroanalytical Chemistry*, *814*, 7 – 19.

Rana, S., Mittal, S. K., Singh, N., Singh, J., & Banks, C. E. (2017). Schiff base modified screen printed electrode for selective determination of aluminium(III) at trace level. *Sensors and Actuators B: Chemical*, *239*, 17 – 27.

Rastogi, L., Dash, K., & Ballal, A. (2017). Selective colorimetric/visual detection of Al^{3+}in ground water using ascorbic acid capped gold nanoparticles. *Sensors and Actuators B*, *248*, 124 – 132.

Sarkar, D., Ghosh, P., Gharami, S., Mondal, T. K., & Murmu, N. (2017). A novel coumarin based molecular switch for the sequential detection of $Al^{3+}$and F^{-}: Application in lung cancer live cell imaging and construction of logic gate. *Sensors and Actuators B: Chemical*, *242*, 338 – 346.

Skalny, A. V., Kaminskaya, G. A., Krekesheva, T. I., Abikenova, S. K., Skalnaya, M. G., Bykov, A. T., & Tinkov, A. A. (2018). Assessment of hair metal levels in aluminium plant workers using scalp hair ICP-DRC-MS analysis. *Journal of Trace Elements in Medicine and Biology*, *50*, 658 – 663.

Siddiquee, S., Yusof, N. A., Salleh, A. B., Tan, S. G., & Bakar, F. A. (2010). Electrochemical DNA biosensor for the detection of Trichoderma harzianum based on a gold electrode modified with a composite membrane made from an ionic liquid ZnO nanoparticles and chitosan, and by using acridine orange as a redox indicator. *Microchimica Acta*, *172*, 357 – 363.

Silva, E. D. N. D., Heerdt, G., Cidade, M., Pereira, C. D., Morgon, N. H., & Cadore, S. (2015). Use of in vitro digestion method and theoretical calculations to evaluate the bioaccessibility of Al, Cd, Fe and Zn in lettuce and cole by inductively coupled plasma mass spectrometry. *Microchemical Journal*, *119*, 152 – 158.

Soni, M. G., White, S. M., Flamm, W. G., & Burdock, G. A. (2001). Safety evaluation of dietary aluminium. *Regulatory Toxicology and Pharmacology*, *33*, 66 – 79.

Suherman, A. L., Tanner, E. E. L., Kuss, S., Sokolov, S. V., Holter, J., Young, N. P., & Compton, R. G. (2018). Voltammetric determination of aluminium(III) at tannic acid capped-gold nanoparticle modified electrodes. *Sensors and Actuators B*, *265*, 682 – 690.

Tarley, C. R., Basaglia, A. M., Segatelli, M. G., Prete, M. C., Suquila, F. A. C., & Oliveira, L. L. G. (2017). Preparation and application of nanocomposite based on imprinted poly(methacrylic acid)-PAN/MWCNT as a new electrochemical selective sensing platform of Pb^{2+} in water samples. *Journal of Electroanalytical Chemistry*, *801*, 114 – 121.

Trachioti, M. G., Hrbac, J., & Prodromidis, M. I. (2018). Determination of Cd and Zn with "green" screen-printed electrodes modified with instantly prepared sparked tin nanoparticles. *Sensors and Actuators B: Chemical*, *260*, 1076 – 1083.

Tripathi, R. M., Gupta, R. K., Singh, P., Bhadwal, A. S., Shrivastav, A., Kumar, N., & Shrivastav, B. R. (2014). Ultra-sensitive detection of mercury(II) ions in water sample using gold nanoparticles synthesized by Trichoderma harzianum and their mechanistic approach. *Sensors and Actuators B: Chemical*, *204*, 637 – 646.

Wang, J. (2001). *Analytical electrochemistry* (2nd ed.). New York: Wiley-VCN.

Wang, C. X., Wu, B., Zhou, W., Wang, Q., Yu, H., Deng, K., Li, J. M., Zhuo, R. X., & Huang, S. W. (2018). Turn-on fluorescent probe-encapsulated micelle as colloidally stable nanochemosensor for highly selective detection of Al^{3+} in aqueous solution and living cell imaging. *Sensors & Actuators: B. Chemical*, *271*, 225 – 238.

Wen, S. H., Wang, Y., Yuan, Y. H., Liang, R. P., & Qui, J. D. (2018). Electrochemical sensor for arsenite detection using graphene oxide assisted generation of Prussian blue nanoparticles as enhanced signal label. *Analytica Chimica Acta*, *1002*, 82 – 89.

World Health Organization. (1998). Guidelines for drinking water quality (Second edition, Volume 2, p. 3). Retrieved from https://www.who.int/water_sanitation_health/dwq/2edaddvol2a.pdf.

Wu, W., Jia, M., Zhang, Z., Chen, X., Zhang, Q., Zhang, W., … Chen, L. (2019). Sensitive, selective and simultaneous electrochemical detection of multiple heavy metals in environment and food using a low cost Fe3O4 nanoparticles/fluorinated multi-walled carbon nanotubes sensor. *Ecotoxicology and Environmental Safety*, *175*, 243 – 250.

Xuan, X., & Park, J. Y. (2018). A miniaturized and flexible cadmium and lead ion detection sensor based on micro-patterned reduced graphene oxide/carbon nanotube/bismuth composite electrodes. *Sensors and Actuators B*, *255*, 1220 – 1227.

Yang, Y., Kang, M., Fang, S., Wang, M., He, L., Zhao, J., … Zhang, Z. (2015). Electrochemical biosensor based on three-dimensional reducedgraphene oxide and polyaniline nanocomposite for selective detection of mercury ions. *Sensors and Actuators B*, *214*, 63 – 69.

Zioła-Frankowska, A., Kuta, J., & Frankowski, M. (2015). Application of a new HPLC-ICP-MS method for simultaneous determination of Al^{3+} and aluminium fluoride complexes. *Heliyon*, e00035. DOI: http://dx.doi.org/10.1016/j.heliyon.2015.e00035